Application of Artificial Intelligence to DFIG based Wind Farm for Reactive Power Compensation

P. Jyothi*, R. B. R. Prakash*‡, P. Srinivasa Varma*

*Department of Electrical and Electronics Engineering, Koneru Lakshmaiah Education Foundation, Vaddeswaram, A.P, India.

(jyothi.polathala@gmail.com, bhanu184@kluniversity.in, pinnivarma@kluniversity.in)

‡ Corresponding Author; R B R Prakash, Department of EEE, Koneru Lakshmaiah Education Foundation, Vaddeswaram, India., Tel: +91 9491952299, bhanu184@kluniversity.in

Received: 22.03.2020 Accepted:20.04.2020

Abstract- Doubly Fed Induction Generators are mainly used in the wind applications. In this paper, a new method for reactive power compensation in wind farms is proposed by using DSTATCOM with the Kohonen Learning neural network (KLNN) based control algorithm. In the proposed control strategy, instantaneous PCC voltages and load currents will be taken into account to estimate the load conductance and susceptance. KLNN will give the required load conductance and susceptance to estimate the reference supply currents. DSTATCOM will be operated as per these reference supply currents. Reactive power compensation will be achieved with the combination of KLNN and DSTATCOM. The proposed approach was examined in the Simulink model in MATLAB.

Keywords- Conductance, Susceptance, DFIG, Reactive power compensation, Neural Network (NN).

1. Introduction

Energy planning involves finding a variety of sources to meet energy needs in the most reliable way. Being a cheap and clean source of energy, wind energy is one of the technologies. Wind farms are dominated by the doubly fed induction generator (DFIG) compared to SCIG due to the greater advantages. Speed can be varied with DFIG, but this requirement is not met with SCIG [1].

The distribution system has mostly non-linear loads and devices are extremely sensitive to deprived voltage quality. Reactive power is used in the inductive and capacitive loads [2]. Considerable reactive power flows throughout a power system is replicated in voltage variations at the point of common coupling because of the reactive impedance of the system.

Power Quality is deteriorating due to the increased use of reactive energy. The growth of fast and reliable semiconductor devices has introduced new electronic power configurations to the responsibilities of power transmission and load flow control. FACTS systems have fast and precise control over transmission parameters [3].

Among the different types of FACTS devices, DSTATCOM is too visible and could be an economical solution to compensate for the reactive vars and unbalanced load on the distribution system. DSTATCOM effectively feeds a current into the system to determine the power factor, reactive vars compensation and harmonic reduction [4]-[6]. Another advantage is the reactive power fed in is independent of the mains voltage at the PCC [6]-[9]. Different types of loads occur in the system. Power supply quality anomalies related to non-linear loads include load imbalance, harmonics, power to weight with high reactivity and voltage fluctuations [10].

Unbalanced and nonlinear loads connected to a four-wire three phase distribution system, which encounters a higher neutral current consisting of fundamental and harmonic frequency components, lead to an overload of the neutral conductor. To compensate for the neutral current, there are different strategies with the help of the use of magnets [11]. In this application, the three-legged VSC (DSTATCOM) is used in conjunction with the transformer connected to T, due to the facets of this configuration. The rating of the transformer connected to T is much lower and also requires two one phase transformers [12].

The 3-leg VSC based DSTATCOM is employed for this application, it implemented by using IGBT's. DSTATCOM's efficiency relies on the algorithm of control used to reap reference currents. There are several types of control algorithms for the DSTATCOM. The different types of control techniques are: PWM, Synchronous PWM, SPWM [13], SVPWM [2], d-q theory, synchronous reference frame, Phase shift control, instantaneous reactive power theory and Neural Network based control algorithms [BP, Hopfield and etc.]. Abhishri Jani and Elijah Toppo have described a control algorithm based on synchronous

PWM[13], Adeesh Sharma and Himmat Singh have investigated control technique based on Space Vector PWM[2], N.H. Baharudina, S.I. Syed Hassan, illustrate the different control algorithms based on NN[14]. Research has shown that neural networks (NN) have the functionality to improve control of the electronic feeding device; therefore, NN with Kohonen Learning Algorithm has been used in this work. The DFIG applications and details are given in [15]-[20].

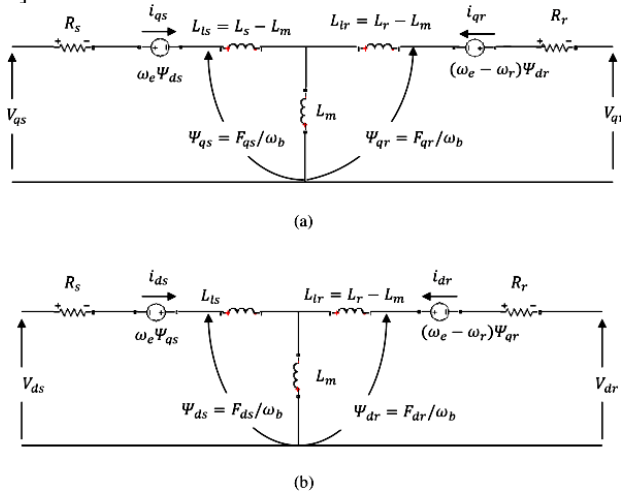

Fig. 1: Equivalent circuit diagram of DFIG for modelling.

As mentioned in the literature survey many control strategies were used to implement the reactive power compensation but in those, reference components taken from the rated values are taken from the desired operation codes. But here these reference values generated from the fundamental parameters; conductance and susceptance.

In this article, an algorithm is implemented that was initiated when evaluating load conductivity using NN in a three-phase DSTATCOM to improve power quality. The algorithm is replicated as Kohonen learning or Kohonen feature maps. This extracts the basic component of the load currents (conductivity and susceptibility). A weighted value for the conductivity or susceptance of their grouped values is proposed, which coincides with the input conductivity, which comes extremely close to the real value as conductivity extraction or susceptance in signal processing for evaluating the reference supply current. This algorithm is best suited for circumstances in which the periodicity of the charges is not constant or the charging currents often vary. This is based on a solid basic circuit theory than the other old-style NN algorithm. This is adopted as follows to meet the proposed control strategy.

For implementing proposed control strategy, initial instantaneous voltages at the point of common coupling is taken and split them into p, q components and parallelly load currents taken. Using these p, q voltages and load currents, instantaneous values of actual load conductance and susceptance are determined. These given to Kohonen Learning algorithm to estimate the required or desired load conductance and susceptance in turn to estimate the reference supply currents. With the KL NN given conductance values, p-components of reference supply currents and from the susceptance values, q-components of reference supply currents were determined. From these two components reference values of supply currents generated. These ref. Supply currents used to control the DSTACOM to regulate the reactive power in the need [28].

This paper is organized as follows. Modelling of DFIG and D-STATCOM is explained in section 2. Section 3 describes the Modelling and working procedure of Kohonen Learning Neural Network control algorithm. Grid connected mode and islanded mode of operation with linear and non linear loads results are described in section 4. Finally, specific important conclusions of this paper are drawn in section 5.

2. DFIG and D-STATCOM Modelling

2.1. DFIG Modelling:

Wind energy from wind turbines is transferred into mechanical power through gear box. This mechanical power is converted into electrical power by means of generator.

DFIG is similar to AC generator but can operate above and below the synchronous speed. It consists of two windings; stator and rotor windings. DFIG Stator is directly connected to the load or grid and rotor windings are connected to the load or grid through back to back Voltage Source Converter. These back to back converters control the rotor and grid currents. The equivalent circuit of DFIG in d and q axes are shown in fig. 1. Eq. (1) to Eq. (5) are useful to model the DFIG.

Stator Voltage:

$$V_{ds} = R_s I_{ds} - \omega_s \varphi_{qs} + \frac{d\varphi_{ds}}{dt} \quad (1)$$

$$V_{qs} = R_s I_{qs} + \omega_s \varphi_{ds} + \frac{d\varphi_{qs}}{dt} \quad (2)$$

Rotor Voltage:

$$V_{dr} = R_r I_{dr} - S\omega_s \varphi_{qr} + \frac{d\varphi_{dr}}{dt} \quad (3)$$

$$V_{qr} = R_r I_{qr} + S\omega_s \varphi_{dr} + \frac{d\varphi_{qr}}{dt} \quad (4)$$

The electromagnetic torque is expressed as:

$$T_e = \frac{3}{2} n_p (\Psi_{ds} I_{qs} - \Psi_{qs} I_{ds}) \quad (5)$$

Where $L_s = L_{ls} + L_m$, $L_r = L_{lr} + L_m$ and $S\omega_s = \omega_s - \omega_r$, L_m is mutual inductance. Suffixes s, r, d and q are stator, rotor, d-axis and q-axis respectively. In order to control the wind turbine output power, the rotor-side converter is used. The rotor-side converter reference current is given by

$$I_{dr-ref} = -\frac{2L_s T_e}{3 n_p L_m \Psi_s} \quad (6)$$

Where n_p is no. of pole pairs. The stator-side converter (Grid-side converter) is primarily used to maintain DC-link voltage [12]-[14].

2.2. D-STATCOM Modelling:

A DSTATCOM based Voltage Sourced Converter (VSC) is linked to 3-phase ac mains feeding three-phase linear/ nonlinear grid impedance loads [21]. The device is realized the use of six IGBT switches with protecting anti-parallel diodes. In tandem with the load and the compensator, an RC filter is connected to the system in order to lessen converting ripples in the PCC voltage added by DSTATCOM switching. Interfacing inductors are employed on the AC side of Voltage Source Converter to limit ripples in current compensation the equivalent circuit for DSTATCOM is shown in fig .2 From equivalent circuit

diagram the differential equations for three-phase are given by

$$\frac{d}{dt}\begin{bmatrix} i'_{pa} \\ i'_{pb} \\ i'_{pc} \end{bmatrix} = \frac{-R'_p\omega_B}{L'_p}.\begin{bmatrix} i'_{pa} \\ i'_{pb} \\ i'_{pc} \end{bmatrix} + \frac{\omega_B}{L'_p}\begin{bmatrix} (v'_{ia} - v'_{pa}) \\ (v'_{ib} - v'_{pb}) \\ (v'_{ic} - v'_{pc}) \end{bmatrix} \quad (7)$$

where i_B is the base value, ω_B is the angular speed at normal frequency. The system is represented as a voltage source ($v'_{pa}, v'_{ib}, \& v'_{ic}$) and is connected to the load through the L'_p and R'_p, which models the losses of the magnetic coupling circuit. DSTATCOM current is denoted as i'_p. The DC circuit is characterized by a current source i'_{dc} linked to the lumped capacitor C'. R'_c indicated semi-conductor and DC-circuit losses.

The DC side current can be given by

$$i'_{dc} = \frac{1}{\omega_B C'}\frac{dv'_{dc}}{dt} + \frac{v'_{dc}}{R'_c} \quad (8)$$

Eq. (9) gives the dc side power of the converter which always equal to the power on the AC side.

$$v'_{dc}i'_{dc} = v'_{pa}i'_{pa} + v'_{pb}i'_{pb} + v'_{pc}i'_{pc} \quad (9)$$

Eq. (10) indicates the modelling equations of the DSTATCOM.

$$\frac{d}{dt}\begin{bmatrix} i'_{pa} \\ i'_{pb} \\ i'_{pc} \\ v'_{dc} \end{bmatrix} = \begin{bmatrix} \frac{-R'_p\omega_B}{L'_p} & 0 & 0 & \frac{-k_p\omega_B}{L'_p}S_a \\ 0 & \frac{-R'_p\omega_B}{L'_p} & 0 & \frac{-k_p\omega_B}{L'_p}S_b \\ 0 & 0 & \frac{-R'_p\omega_B}{L'_p} & \frac{-k_p\omega_B}{L'_p}S_c \\ k_p\omega_B C' S_a & k_p\omega_B C' S_b & k_p\omega_B C' S_c & -\frac{\omega_B C'}{R'_c} \end{bmatrix}\begin{bmatrix} i'_{pa} \\ i'_{pb} \\ i'_{pc} \\ v'_{dc} \end{bmatrix} + \frac{\omega_B}{L'_p}\begin{bmatrix} v'_{ia} \\ v'_{ib} \\ v'_{ic} \\ 0 \end{bmatrix} \quad (10)$$

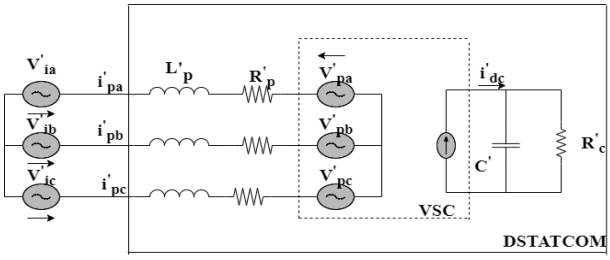

Fig. 2: Equivalent circuit diagram of DSTATCOM.

The DSTATCOM modelled in d-q reference frame is given by

$$\frac{d}{dt}\begin{bmatrix} i'_{pd} \\ i'_{pq} \end{bmatrix} = \begin{bmatrix} \frac{-R'_p\omega_B}{L'_p} & \omega \\ -\omega & \frac{-R'_p\omega_B}{L'_p} \end{bmatrix}\begin{bmatrix} i'_{pd} \\ i'_{pq} \end{bmatrix} + \frac{\omega_B}{L'_p}\begin{bmatrix} (v'_{id} - v'_{pd}) \\ (v'_{iq} - v'_{pq}) \end{bmatrix} \quad (11)$$

From power balance equation

$$i'_{dc} = \frac{3}{2}\left(k_p S_d i'_{pd} + k_p S_q i'_{pq}\right) \quad (12)$$

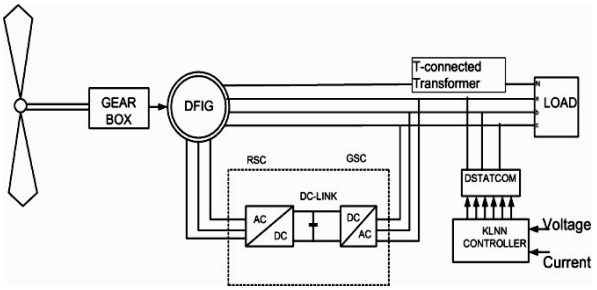

Fig. 3: Proposed Block Diagram.

3. Proposed Control Algorithm

Fig. 3 shows the Block diagram of proposed circuit. Fig. 4 shows the block diagram for extraction of reference currents based on load conductance and susceptance. Three phase VSC based DSTATCOM is employed for this application. PCC voltages (v_{sa}, v_{sb}, v_{sc}), load currents (i_{La}, i_{Lb}, i_{Lc}) and the dc link voltage (v_{dc}) are required for this algorithm to extract currents (i_{sa}^*, i_{sb}^*, i_{sc}^*). Band Pass (BP) filter eliminates the noise and harmonics existing in the PCC voltages in case of distorted ac mains. To limit the disturbances in PCC voltages, these are processed through LPF as

$$V_{ta} = \sqrt{\left[2\left(\frac{v_{sa}{}^2}{2}\right)\right]} \quad (13)$$

$$V_{tb} = \sqrt{\left[2\left(\frac{v_{sb}{}^2}{2}\right)\right]} \quad (14)$$

$$V_{tc} = \sqrt{\left[2\left(\frac{v_{sc}{}^2}{2}\right)\right]} \quad (15)$$

where: $v_{sa} = V_{sa}\sin\omega t$; $v_{sb} = V_{sb}\sin(\omega t - 2\pi/3)$, $v_{sc} = V_{sc}\sin(\omega t - 4\pi/3)$.

V_{ta}, V_{tb} and V_{tc} are the constant PCC voltages. These voltages are bought by means of processing through the LPF.

$$u_{ap} = \frac{v_{sa}}{V_{ta}}, u_{bp} = \frac{v_{sb}}{V_{tb}}, u_{cp} = \frac{v_{sc}}{V_{tc}} \quad (16)$$

The magnitude of v_{tp} at PCC is calculated as

$$v_{tp} = \sqrt{\left[2\left(\frac{v_{sa}{}^2 + v_{sb}{}^2 + v_{sc}{}^2}{3}\right)\right]} \quad (17)$$

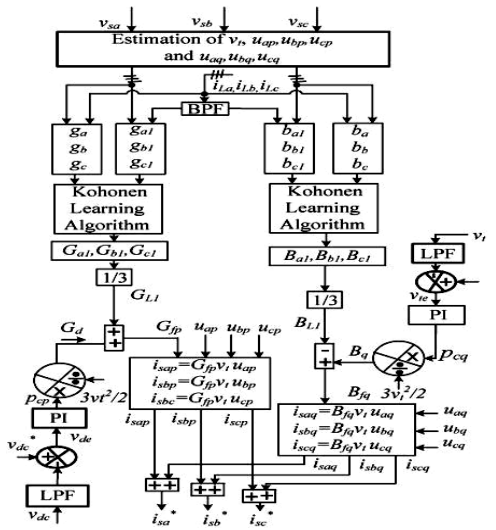

Fig. 4: Estimation of reference supply currents using load conductance & susceptance.

The PCC voltages have fundamental negative sequence voltage due to this the amplitude v_{tp} may also have the ripples in it. To gain the fundamental positive sequence PCC voltages, the v_{tp} is processed thru the LPF and is represented with the aid of v_t. Normally, apparent power is calculated with the aid of the use of p_t, q_t is given by

$$s_a = p_{ta} + q_{ta} \quad (18)$$

The $g_a, g_b, and\ g_c$ are calculated as given by

$$g_a = \frac{p_{ta}}{(v_{ta})^2} \quad (19)$$

$$g_b = \frac{p_{tb}}{(v_{tb})^2} \quad (20)$$

$$g_c = \frac{p_{tc}}{(v_{tc})^2} \quad (21)$$

where $p_{ta} = v_t u_{ap} i_{La}$, $p_{tb} = v_t u_{bp} i_{Lb}$ and $p_{tc} = v_t u_{cp} i_{Lc}$. To calculate the instantaneous basic values of the load conductance's (g_{a1}, g_{b1}, g_{c1}), the BPF currents and voltages at the PCC are used. The G_{a1}, G_{b1}, G_{c1} are calculated by way of applying kohonen algorithm to g_a, g_b, g_c and g_{a1}, g_{b1}, g_{c1}. The fundamental load conductance's are updated at r[th] sampling instant is given by

$$G_{a1} = g_{a1}(r+1) = g_{a1}(r) - \tau\{g_a(r) - g_{a1}(r)\} \quad (22)$$

Similarly, G_{b1} & G_{c1}. Where $(g_a - g_{a1})$ is non-fundamental quantity present in the conductance.

The learning rate (τ) rate of the algorithm decides its performance. In this application the best value found is 0.11 and this may be varying between 0 and 1. After many iterations, the unique values of G_{a1}, G_{b1}, G_{c1} are obtained. The flow chart for the kohonen algorithm is given in the following fig. 5.

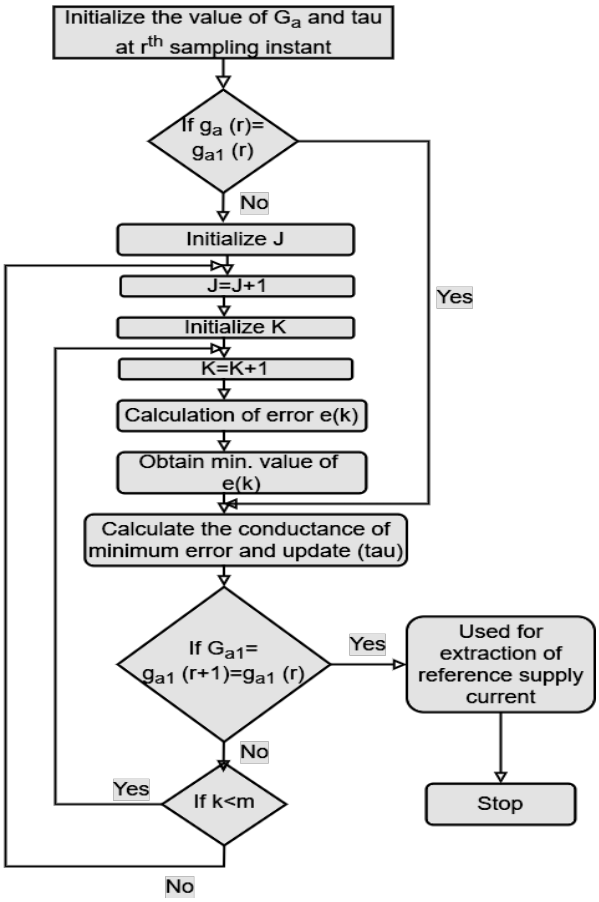

Fig. 5: Flow chart for phase "a" conductance.

If there are any unbalances in the load due to some reasons, in this situation also want to sustain balanced source currents for this purpose the G_{L1} is calculated and it is given by

$$G_{L1} = \frac{G_{a1}+G_{b1}+G_{c1}}{3} \quad (23)$$

The difference between $v_{dc}{}^*$ and v_{dc} are calculated and it is used for error voltage at r[th] sampling instant is given by

$$v_{de}(r) = v_{dc}{}^*(r) - v_{dc}(r) \quad (24)$$

The VSC dc link voltage is delimited with the aid of capability of a PI controller. This Proportional Integral controller placed in dc-link for voltage purpose, the output of this utilized upholding DSTATCOM's voltage of dc-link is given by

$$p_{cp}(r) = p_{cp}(r-1) + k_{dp}\{v_{de}(r) - v_{de}(r-1)\} + k_{di} v_{de} \quad (25)$$

The $p_{cp}(r)$ is used as p_{cp} to keep away from difficulties in calculations. These components are used for compensating the active power losses present in the Voltage Source Converter. The dc-link voltage controller output p_{cp} correspondent conductance (G_d) is calculated by using below formulae

$$G_d = \frac{2p_{cp}}{3{v_t}^2} \quad (26)$$

The total conductance corresponding to the supply active power is given by

$$G_{fp} = G_d + G_{L1} \quad (27)$$

The in-phase extracted reference current components are estimated as

$$i_{sap} = G_{fp} v_t u_{ap} \quad (28)$$

$$i_{sbp} = G_{fp} v_t u_{bp} \quad (29)$$

$$i_{scp} = G_{fp} v_t u_{cp} \quad (30)$$

The quadrature unit templates are estimated as

$$u_{aq} = \frac{(-u_{bp}+u_{cp})}{\sqrt{3}} \quad (31)$$

$$u_{bq} = \frac{(3u_{ap}+u_{bp}-u_{cp})}{2\sqrt{3}} \quad (32)$$

$$u_{cq} = \frac{(-3u_{ap}+u_{bp}-u_{cp})}{2\sqrt{3}} \quad (33)$$

The $b_a, b_b, and\ b_c$ are calculated as

$$b_a = \frac{q_{ta}}{(v_{ta})^2}\ ;\ b_b = \frac{q_{tb}}{(v_{tb})^2}\ ;\ b_c = \frac{q_{tc}}{(v_{tc})^2} \quad (34)$$

where: $q_{ta} = v_t u_{aq} i_{La}$, $q_{tb} = v_t u_{bq} i_{Lb}$ and $q_{tc} = v_t u_{cq} i_{Lc}$.The susceptance $(b_{a1}, b_{b1,}$ and $b_{c1})$ is calculated by placing BPF in load side currents and the voltages at PCC.

The susceptance (B_{a1}, B_{b1}, B_{c1}) are calculated by applying kohonen algorithm to b_a, b_b, b_c and b_{a1}, b_{b1}, b_{c1}. The fundamental load susceptance are updated at r[th] sampling instant is given by

$$B_{a1} = b_{a1}(r+1) = b_{a1}(r) - \tau\{b_a(r) - b_{a1}(r)\}$$

$$B_{b1} = b_{b1}(r+1) = b_{b1}(r) - \tau\{b_b(r) - b_{b1}(r)\}$$

$$B_{c1} = b_{c1}(r+1) = b_{c1}(r) - \tau\{b_c(r) - b_{c1}(r)\} \quad (35)$$

where $(b_a - b_{a1})$, $(b_b - b_{b1})$ and $(b_c - b_{c1})$ are nonfundamental quantity of susceptance.

The flow chart for Kohonen algorithm training of phase "a" is shown in fig.5. To calculate B_{a1}, B_{b1} and B_{c1} same algorithm will be used. The B_{L1} is calculated as

$$B_{L1} = \frac{B_{a1}+B_{b1}+B_{c1}}{3} \quad (36)$$

Eq. (37) gives the error voltage (v_{te}) is calculated by taking the difference of the $v_t^*(r)$ and $v_t(r)$ at the r[th] iteration or sampling instant.

$$v_{te}(r) = v_t^*(r) - v_t(r) \quad (37)$$

Eq. (38) gives the PI controller output voltage $p_{cq}(r)$ which maintains the PCC voltage at constant. Eq. (38) written for the r[th] sampling instant.

$$p_{cq}(r) = p_{cq}(r-1) + k_{tp}\{v_{te}(r) - v_{te}(r-1)\} + k_{ti}v_{te}(r) \quad (38)$$

The (B_q) related to p_{cq} is calculated as

$$B_q = \frac{2p_{cq}}{3{v_t}^2} \quad (39)$$

The susceptance corresponding to the source reactive power is given by

$$B_{fq} = B_q - B_{L1} \quad (40)$$

Eq. (41) to (43) shows the estimated quadrature components of the reference source currents.

$$i_{saq} = B_{fq}v_t u_{aq} \quad (41)$$

$$i_{sbq} = B_{fq}v_t u_{bq} \quad (42)$$

$$i_{scq} = B_{fq}v_t u_{cq} \quad (43)$$

The final extracted currents are given by

$$i_{sa}^* = i_{sap} + i_{saq} \quad (44)$$

$$i_{sb}^* = i_{sbp} + i_{sbq} \quad (45)$$

$$i_{sc}^* = i_{scp} + i_{scq} \quad (46)$$

The estimated reference source currents and sensed source currents are compared, the error is amplified through the PI controller. The PI controller output is given as input for PWM generator to generate triggering pluses for IGBT's of DSTATCOM. This method also known as indirect extraction of current error components. In this method the in-phase component of the reference source currents are used in Power Factor Correction mode to trigger the IGBT switches[22] & [24].

4. Simulation Outcomes and Analysis

The proposed controlling method has tested in MATLAB/SIMULINK. The simulation has done for DFIG based wind farm with grid connected mode and islanded mode with linear and non-linear loads. The linear loads are realized by using resistance (R) and inductance (L) and non-linear loads are realized by introducing power electronic devices (in this, diodes are used). The proposed control algorithm for DSTATCOM has tested. The following fig. 6 shows the simulation diagram for linear loads in grid connected mode.

4.1. Grid-Connected mode of Linear Load:

Fig. 6 shows the simulation model for the linear balanced loads. The DSTATCOM realized by IGBT's and interfacing inductor L_{fa}, is used for smoothing the waveform. To filter out the ripples in the system the resistance (R_{fa}) and capacitance (C_{fa})are used. To create the unbalance in the system phase "a" load is removed at 0.151 sec. under this situation the supply currents are balanced it can be observed from fig. 7.

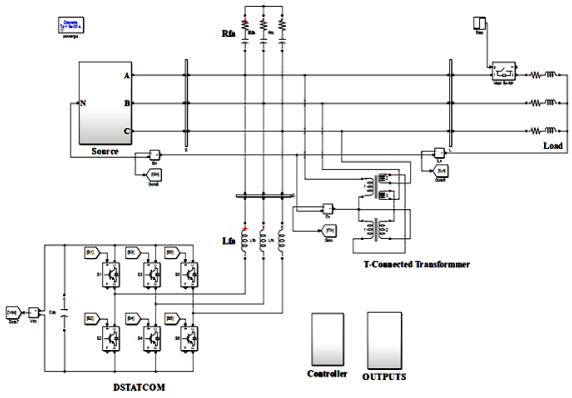

Fig. 6: Simulation diagram of grid-connected mode for line load.

The active power waveforms of DFIG, grid, load and DSATCOM are shown in above fig. 8. The active powers are 424 W, 160 W, 441 W and 143W of DFIG, grid, load and DSTATCOM respectively. The combined active power of wind turbine and grid is 584 W and the load required active power is 441W and the remaining amount of active power 143W is utilized by DSTATCOM to provide reactive power to the load.

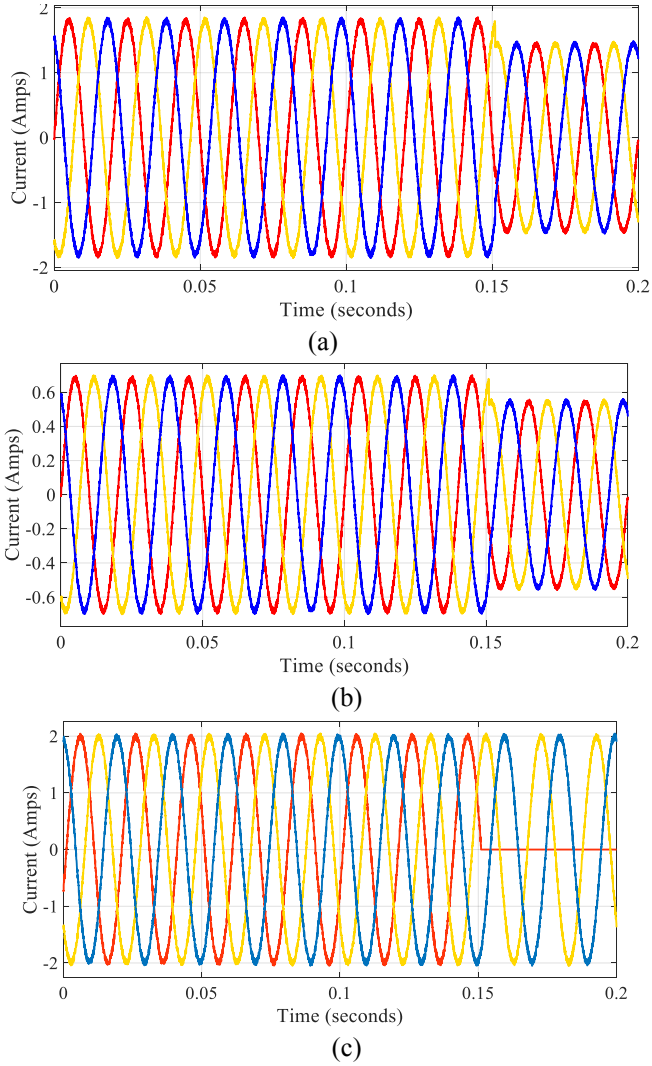

Fig. 7: Current waveform of grid-connected mode for linear load. (a) DFIG current (b) Grid Current (c) Load Current

The reactive power waveforms of DFIG, grid, load and DSATCOM are shown in above fig. 9. The reactive powers are 0.04VAR, 0.01VAR, 161VAR and 160.95VAR of DFIG, grid, load and DSTATCOM. The combined reactive power of DFIG and grid is 0.05VAR. But the load required reactive power is 161VAR it clearly shown in the fig. 9. The load required reactive power is given by the DSTATCOM (160.95VAR).

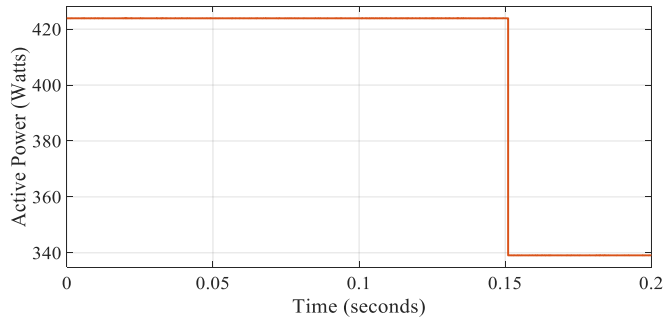

(a)

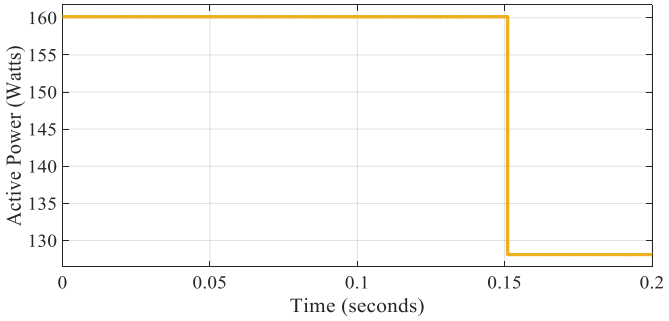

(b)

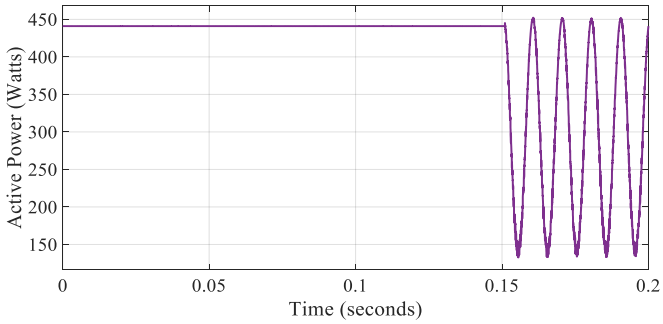

(c)

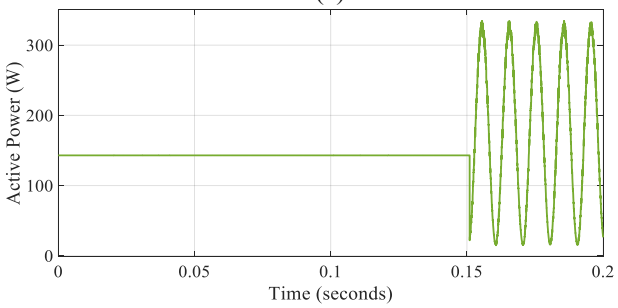

(d)

Fig. 8: Active Power waveform of grid-connected mode for linear load. (a) DFIG Active power (b) Grid Active power (c) Load Active power (d) DSTATCOM Active power

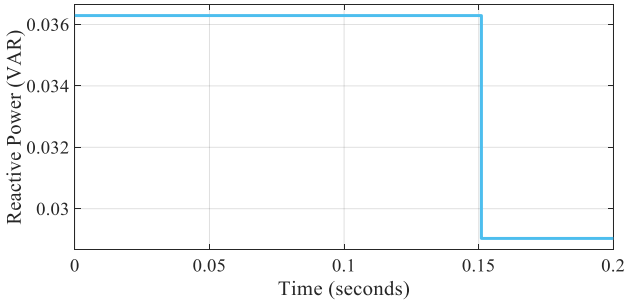

(a)

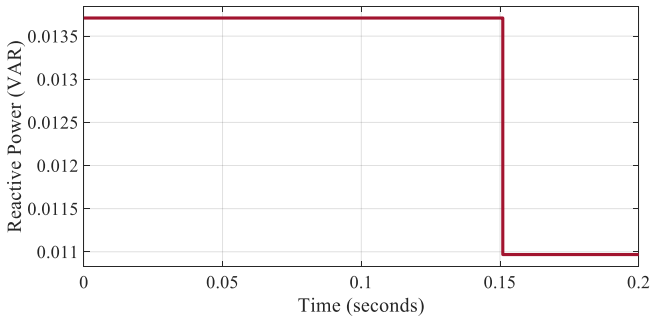

(b)

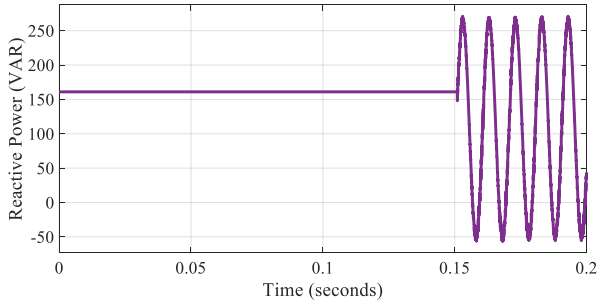

(c)

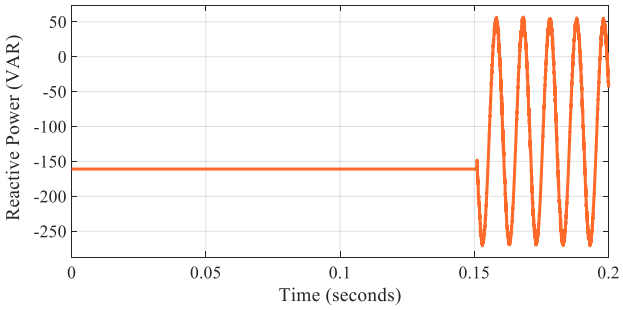

(d)

Fig.9: Reactive Power waveform of grid-connected mode for linear load. (a) DFIG Reactive power (b) Grid Reactive power (c) Load Reactive power (d) DSTATCOM Reactive power

4.2. Grid-Connected mode of Non-Linear Load:

The non-linear loads are realized by introducing diodes. The fig. 10 shows the current waveforms of DFIG, grid, load and fig. 11 shows the active power waveform of DFIG, grid, load and DSTATCOM respectively. Fig. 12 shows the reactive power waveform of DFIG, grid, load and DSTATCOM respectively for non-linear loads.

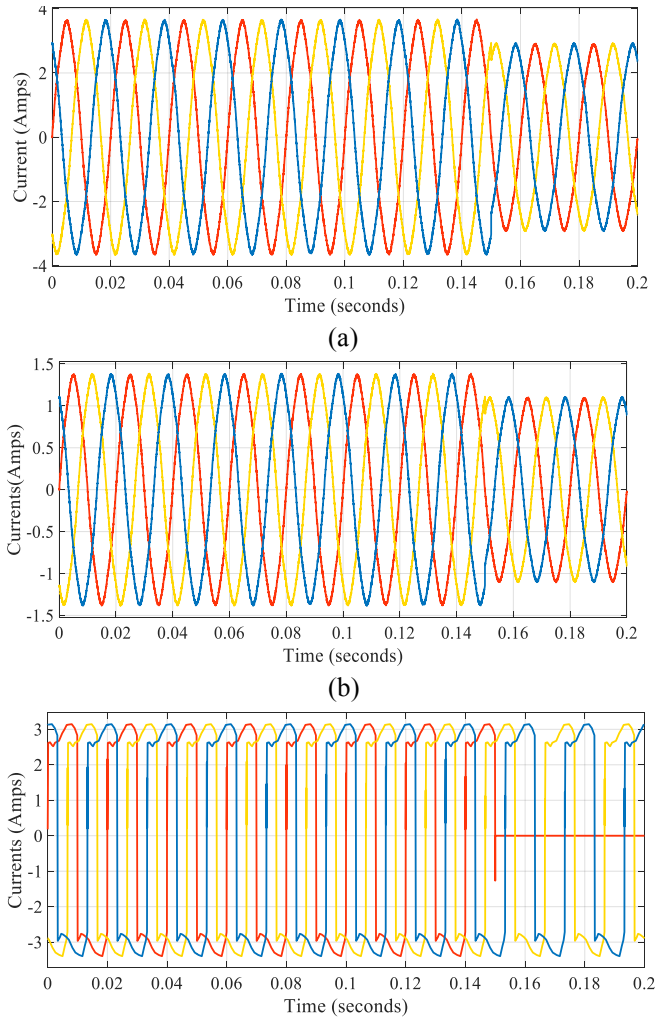

Fig. 10: Current waveform of grid-connected mode for non-linear load. (a) DFIG Currents (b) Grid Currents (c) Load currents

In this also to create a situation like unbalanced load the phase "a" is removed, under this the supply currents are balanced this shown in fig. 10. The total supply active power is 779.9W which contributed by DFIG based wind turbine (566W) and Grid (213.8W) and the DSTATCOM required power is 168W and the remaining power is fed to load (611.9W) which observed in fig. 11.

The reactive power demanded by the load is 175.5VAR, but the reactive power given by the source (combination of Wind Turbine and Grid) is only 13.51VAR. The remaining reactive power is given by the DSTATCOM (162VAR) to load to maintain the voltage profile is shown in fig. 12, fig. 13 shows the harmonic spectrums. The supply voltages of phase "a" voltage (v_{sa})has 2.02% and 2.95% for phase "a" current (i_{sa}). The load voltages of phase "a" voltage has (v_{La}) 2.02% and 44.52% for (i_{La}).

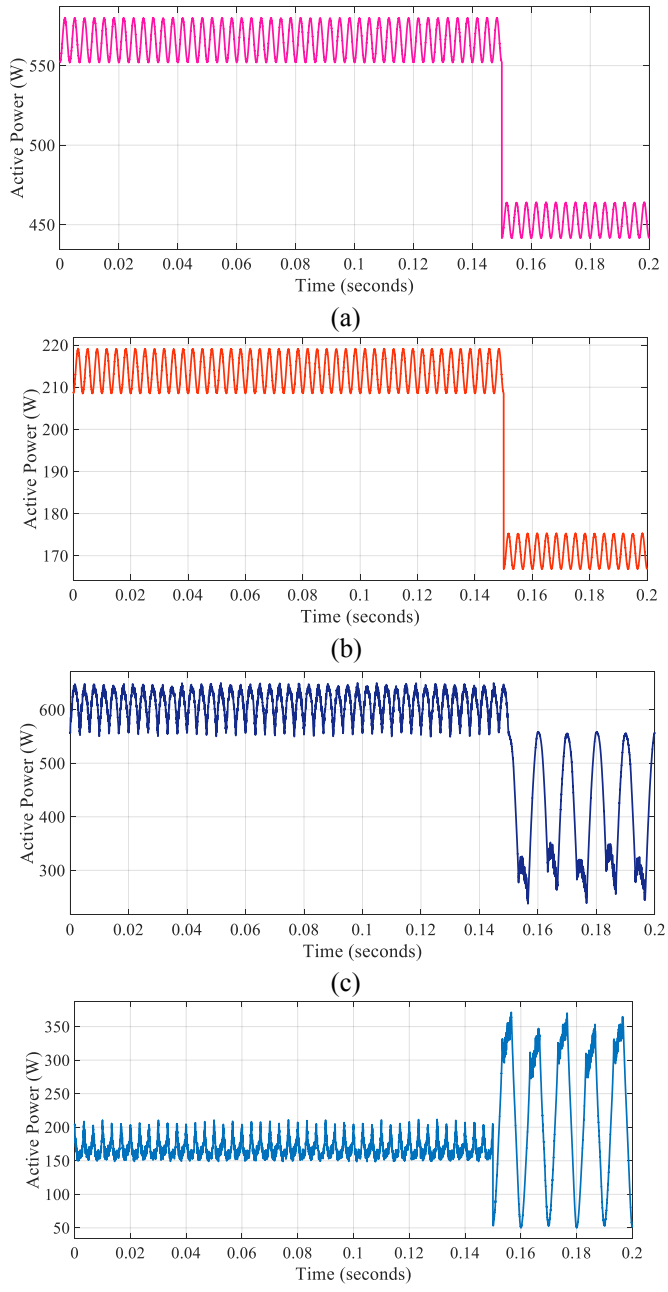

Fig. 11: Active Power waveform of grid-connected mode for non-linear load. (a) DFIG Active power (b) Grid Active power (c) Load Active power (d) DSTATCOM Active power

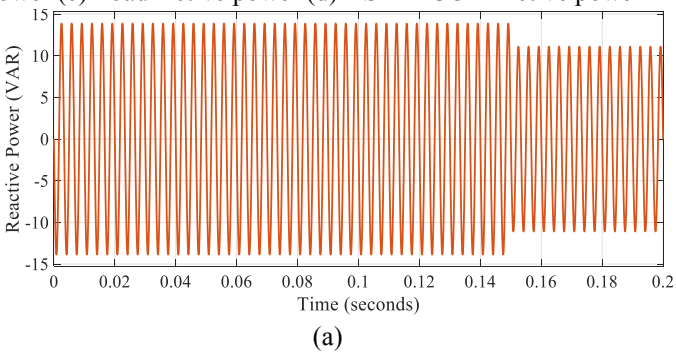

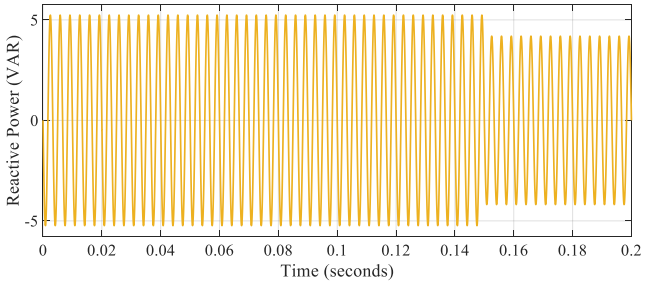

(b)

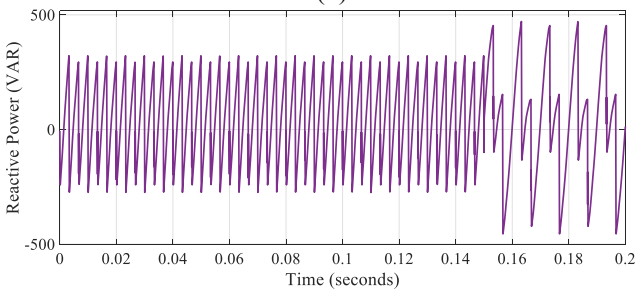

(c)

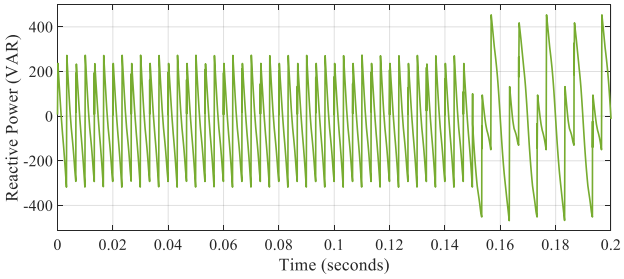

(d)

Fig. 12: Reactive Power waveform of grid-connected mode for non-linear load. (a) DFIG Reactive power (b) Grid Reactive power (c) Load Reactive power (d) DSTATCOM Reactive power

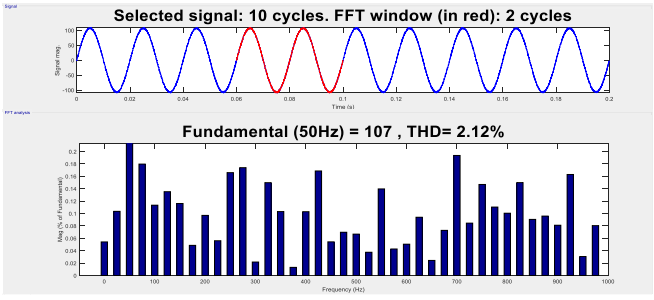

(a)

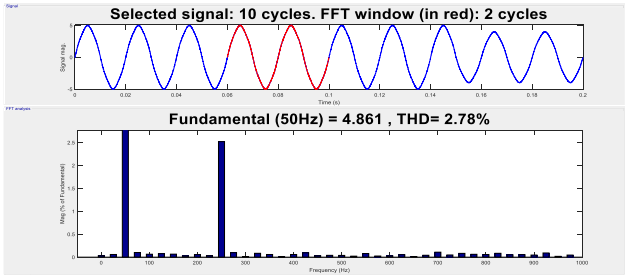

(b)

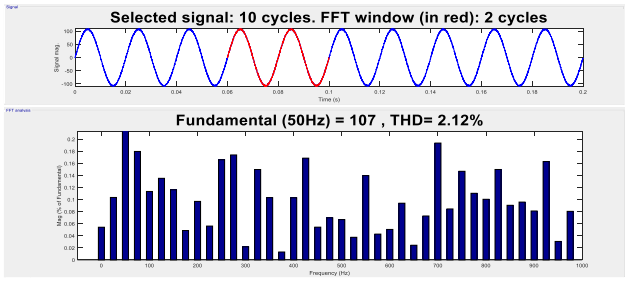

(c)

Fig. 13: Harmonic spectrum of (a) vsa (b) isa (c) vla

4.3. Islanded Mode of Linear Load:

In this mode the grid connection is removed. The behavior of the system can be observed through the waveforms. The source, load and DSTATCOM currents are shown in fig. 14. Under unbalanced load conditions also the supply currents are balanced it can be observed from the waveforms. The amount of active powers is 780W, 611W and 169W of Wind turbine, load and DSTATCOM respectively, this can observe through fig. 15.

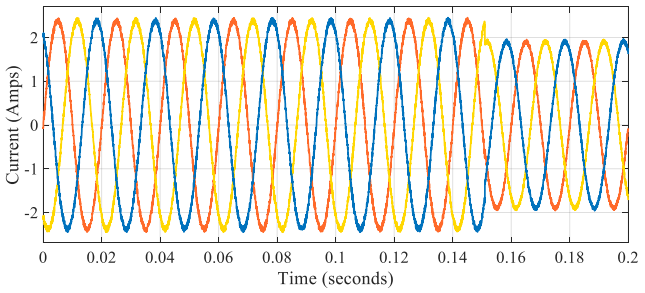

(a)

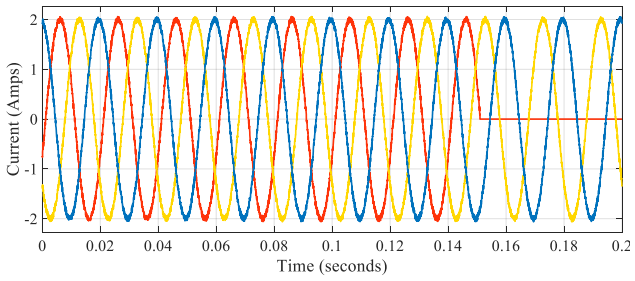

(b)

Fig.14: Current waveform of islanded mode for linear load. (a) wind turbine currents (b) Load currents

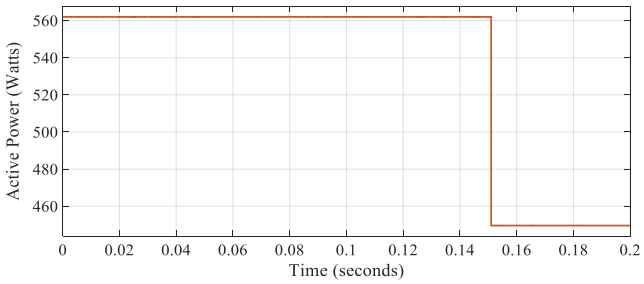

(a)

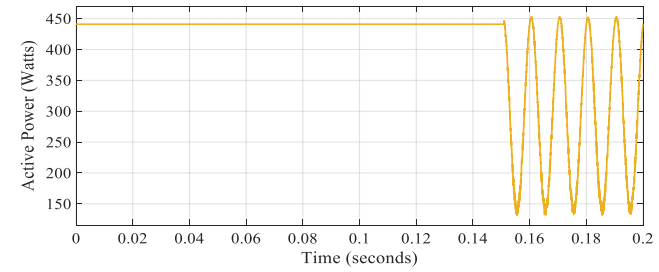

(b)

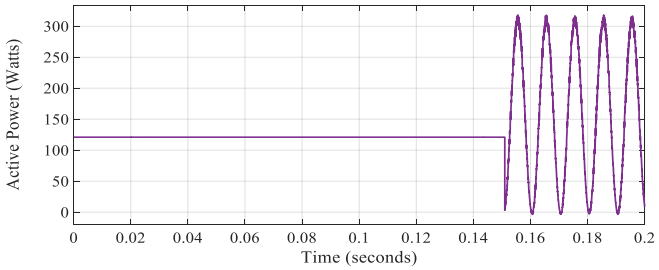

(c)

Fig.15: Active Power waveform of islanded mode for linear load. (a) DFIG Active power (b) Load Active power (c) DSTATCOM Active power

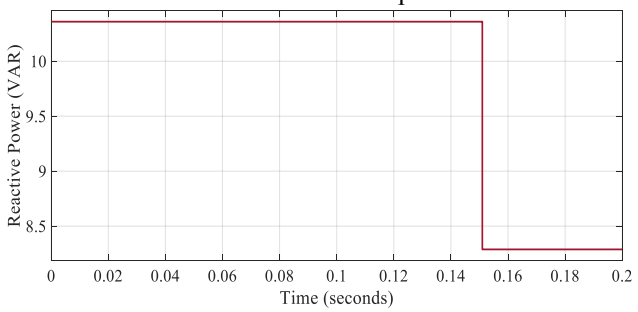

(a)

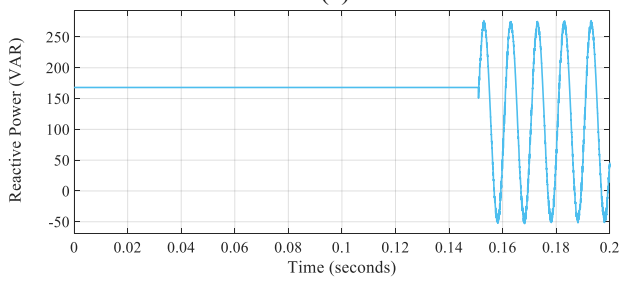

(b)

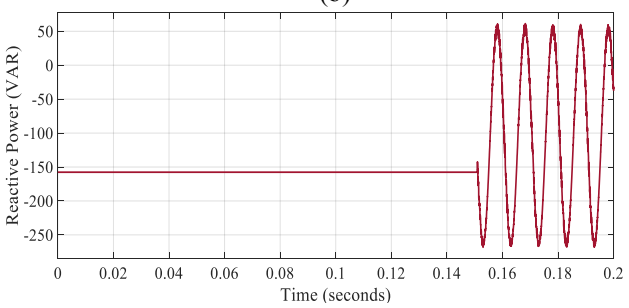

(c)

Fig. 16: Reactive Power waveform of islanded mode for linear load. (a) DFIG Reactive power (b) Load Reactive power (c) DSTATCOM Reactive power

The reactive powers are 15.71VAR, 184.9VAR and 169.2VAR of wind turbine, load and DSTATCOM. The load requires more amount of reactive power hence the DSTATCOM gives required amount of reactive power to the load.

4.4. Islanded Mode of Non-Linear Load:

In this also the non-linear load is realized by introducing diodes into the circuit. The changes in the currents, active powers and reactive powers can be observed by the waveforms that are presented in this section.

The neutral compensation can observe from the fig. 20 it shows for nonlinear load under islanded mode. Load neutral current (i_{Ln}) is compensated by T-connected transformer neutral current (i_{Tn}). The (i_{Ln}) for compensation is achieved similarly for linear loads under Grid-connected mode and islanded mode. The (i_{Tn}) is equal and out of phase of (i_{Ln}). The T-connected transformer details can be found on [9],[10], & [22].

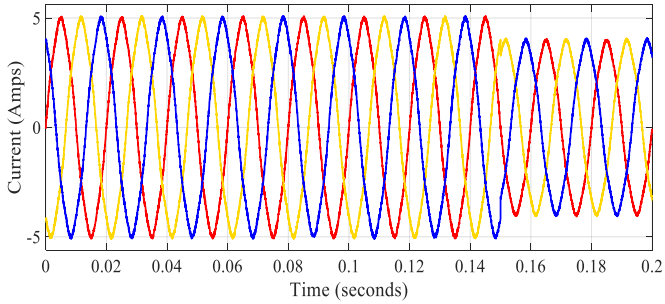

(a)

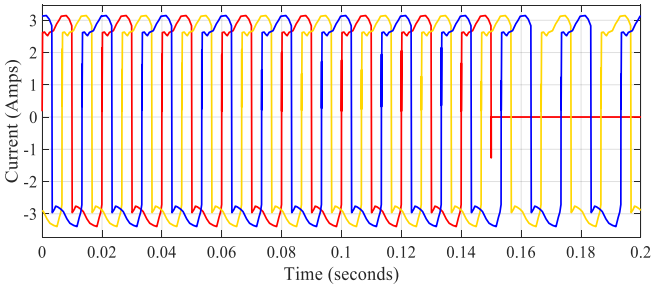

(b)

Fig. 17: Islanded mode of current waveform for non-linear load. (a) DFIG currents (b) Load currents

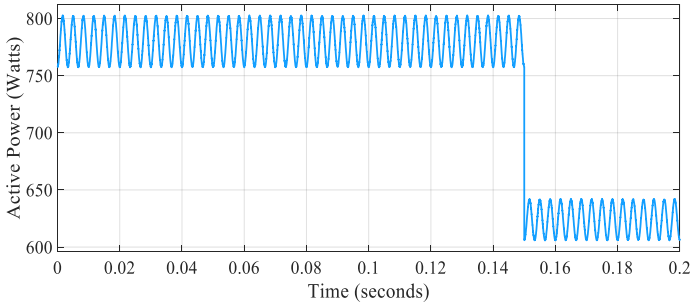

(a)

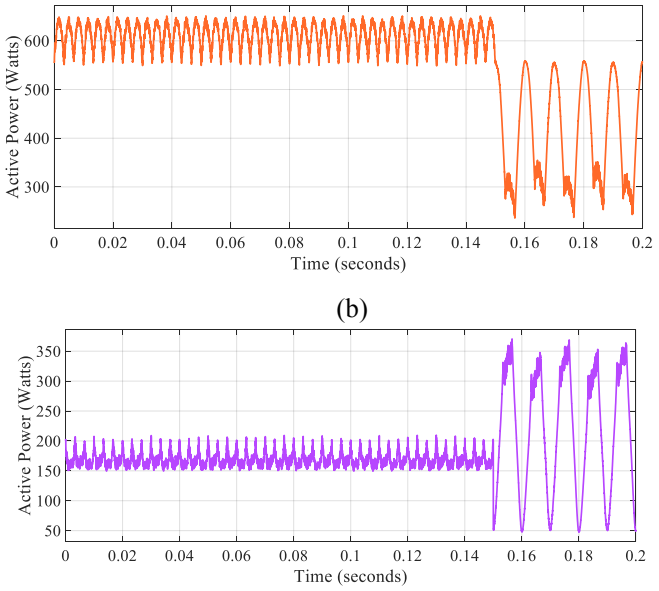

Fig.18: Islanded mode of active power waveform for non-linear load. (a) DFIG Active power (b) Load Active power (c) DSTATCOM Active power

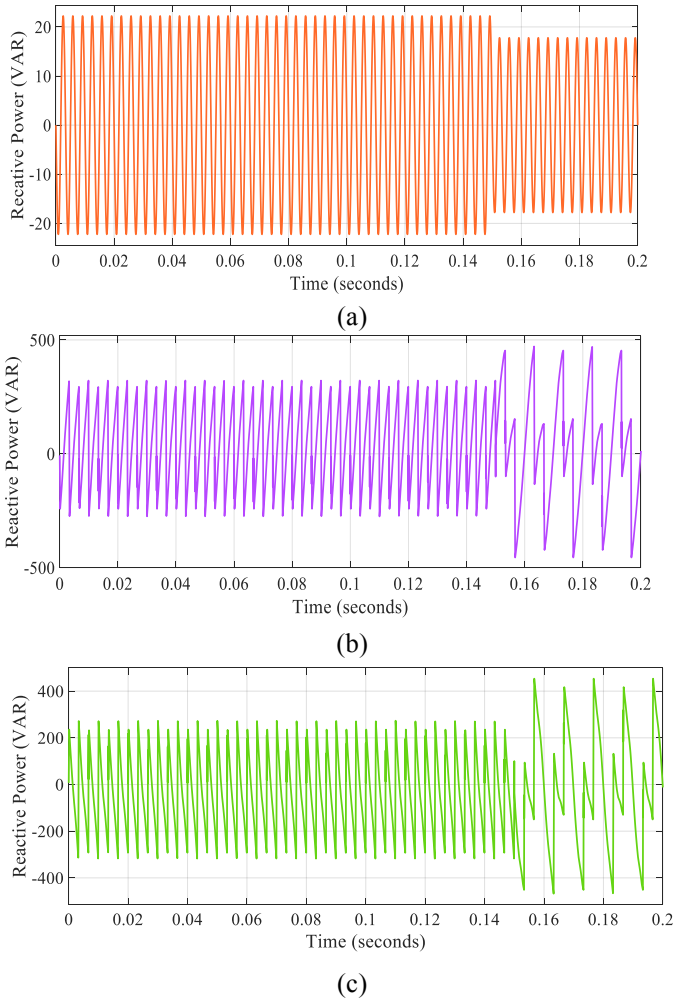

Fig.19: Islanded mode of reactive power waveform for non-linear load. (a) DFIG Reactive power (b) Load Reactive power (c) DSTATCOM Reactive power

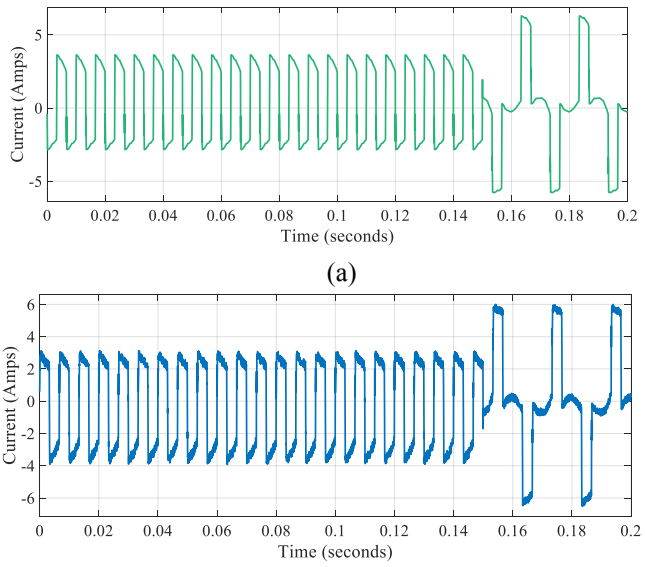

Fig. 20: Neutral Current compensation. (a) Load Neutral current (b) T connected transformer current

5. Conclusion

This simulates the wind turbine based on DFIG and for the control of the DSTATCOM a supervision algorithm is carried out aimed at estimating the conductivity of the load through the Kohonen learning neural network algorithm. DSTATCOM is designed by using three-prong VSC along with a T-connected transformer used to compensate for neutral current. As proposed load instantaneous conductance and susceptance values extracted from line voltages and load currents. Reference supply currents using neural network based conductance based control algorithm are estimated. With these references supply currents firing pulses generated and DSTATCOM operated successfully. From this model in addition to the reactive power compensation, other issues; harmonic reduction and neutral current compensation are addressed. The results show that under unbalanced supply conditions the load currents are also balanced.

References

[1] D. Zhou, Y. Song and F. Blaabjerg, "Modeling and Stress Analysis of Doubly-Fed Induction Generator during Grid Voltage Swell," IEEE, 2016.

[2] A. Sharma and H. Singh, "Matlab Simulation of DSTATCOM using SVPWM," IJETMR, Vol.5, May 2018.

[3] K. Murugesan and R. Muthu, "Modeling and simulation of DSTATCOM for voltage regulations'" 1st International Conference on Electrical Energy Systems, 2011.

[4] Y. Xu, S. Zhao, Y. Cao and K. Sun, "Understanding Subsynchronous Oscillations in DFIG-Based Wind Farms Without Series Compensation," in IEEE Access, vol. 7, pp. 107201-107210, 2019.

[5] K.S.Teja, R B R Prakash, "Power quality improvement using custom power devices in squirrel cage induction generator wind farm to weak-grid connection by using neuro-fuzzy control", International Journal of Power Electronics and Drive System (IJPEDS) Vol. 5, No. 4, April 2015, pp. 477-485.

[6] H. Singa, Ch Sai Ram, R B R Prakash, P Srinivasa Varma, "Fault Diagnosis and Rectification of a DFIG using Multi-Layer Perceptron Control Strategy" International Journal of Innovative Technology and Exploring Engineering (IJITEE), Volume-8 Issue-7 May, 2019, pp 3023-3026.

[7] N. Li, L. Wang, H. Yang and H. Ma, "Stability Analysis for SSR of DFIG-Based Wind Farm Considering STATCOM Capacity Constraint," 2019 22nd International Conference on Electrical Machines and Systems (ICEMS), Harbin, China, 2019, pp. 1-6.

[8] M. J. Morshed and A. Fekih, "A Coordinated Controller Design for DFIG-Based Multi-Machine Power Systems," in IEEE Systems Journal, vol. 13, no. 3, pp. 3211-3222, Sept. 2019.

[9] A. Sharma, "Review Paper on Applications of D-Statcom in Distribution System," IJISME, vol.2, issues 11, Oct 2014.

[10] M. A. H. Sadi, H. Zheng and M. H. Ali, "Transient Stability Enhancement of Power Grid by Neural Network Controlled BFCL Considering Cyber-Attacks," IEEE, 2017.

[11] B. Singh, P. Jayaprakash and D. P. Kothari, "A T-Connected Transformer and Three-leg VSC Based DSTATCOM for Power Quality Improvement", IEEE Transactions on Power Electronics, vol. 23, no. 6, pp. 2710-2718, Nov. 2008

[12] B. Singh, P. Jayaprakash and D. P. Kothari, "Magnetics for Neutral Current Compensation in Three-phase four-wire Distribution System", in Proc. Joint Int. Conf. Power Electron., Drives energy Syst. Power India, 2010, pp. 1-7.

[13] A. Jani and E. Toppo, "Simulation of DSTATCOM for Reactive Power Compensation", IJRED, Recent Trends in Electrical and Electronics & Communication Engineering, pg.no. 33-40, April 2016.

[14] N. H. Baharudin, I. S. H. Syed, P. Saad, P., T. Muhammad, N. T. Mansur & R. Ali, "A Review on DSTATCOM Neural Network Control Algorithm for Power Quality Improvement", Applied Mechanics and Materials, Vol. 785, pp 363-367, 2015.

[15] N. Ullaha, Yong-Taek Oh, "Mathematical Modelling and Simulation of DFIG Wind Turbine and Comparison with Industrial Data", American Scientific Research Journal for Engineering, Technology and Sciences (ASRJETS), Volume 14, No 1, pp 236-249, 2015.

[16] K. L. Shenoy, C. G. Nayak, & R. P Mandi, "Modelling and Performance study of DFIG for Wind Application", International Conference on Smart Technology for Smart Nation, 2017.

[17] G. K. Suman, S. K. Sethi, B.D. Subudhi, "modelling of double fed induction generator connected with wind turbine".

[18] Y. Z. M., Elbuluk, & Yilmaz Sozer, "A Complete Modelling and Simulation of Induction Generator Wind Power Systems", IEEE, 2010.

[19] T. M. Masaud, and P. K. Sen, "modelling and control of doubly fed induction generator for wind power".

[20] A. W. Manyonge, R. M. Ochieng, F. N. Onyango and J. M. Shichikha, "Mathematical Modelling of Wind Turbine in a Wind Energy Conversion System: Power Coefficient Analysis", Applied Mathematical Sciences, Vol. 6, 2012, no. 91, 4527 - 4536.

[21] L. Wang, C. Chang, B. Kuan and A. V. Prokhorov, "Stability Improvement of a Two-Area Power System Connected With an Integrated Onshore and Offshore Wind Farm Using a STATCOM," in IEEE Transactions on Industry Applications, vol. 53, no. 2, pp. 867-877, March-April 2017.

[22] M. Eremia, Chen-Ching Liu, & Abdel-Aty Edris, "Advanced Solutions in Power Systems".

[23] S. Raj Arya and Bhim Singh, "Neural Network Based Conductance Estimation Control Algorithm for Shunt Compensation", IEEE Transactions on Industrial Informatics, Vol. 10, NO. 1, February 2014.

[24] L. Zhizhen, Z. Yan and Z. Xin, "A detecting approach of harmonic currents based on the circuit model and neural network theory," in Proc. Fourtieth IAS Annu. Meet. 2005, pp. 1904–1907.

[25] L. Fausett, "Fundamentals of Neural Networks: Architectures", Algorithms and Applications. Delhi, India: Person Education Asia, 2005.

[26] J. S. R. Jang, C. T. Sun and E. Mizutani, Neuro Fuzzy and Soft Computing: A Computational Approach to Learning and Machine Intelligence. Delhi, India: Person Education Asia, 2008.

[27] B. Singh, and S. Sharma, Member, IEEE, "Design and Implementation of Four-Leg Voltage Source-Converter Based VFC for Autonomous Wind Energy Conversion System," IEEE Transactions on Industrial Electronics, Vol. 59, NO. 12, December 2012.

[28] Z. Rafiee, M. Rafiee, M. Aghamohammadi, "A New Control Strategy based on Reference Values Changing for Enhancing LVRT capability of DFIG in Wind Farm", International Journal of Renewable Energy Research, Vol 9, No 4, pp 1626-1637, Dec 2019.

[29] D. S. Koussa, A. Djoudi and M. Koussa, "Analysis for grid connected wind power system in the arid

region," IREC2015 The Sixth International Renewable Energy Congress, Sousse, 2015, pp. 1-5.

[30] V. Cocina, P. Di Leo, M. Pastorelli and F. Spertino, "Choice of the most suitable wind turbine in the installation site: A case study," 2015 International Conference on Renewable Energy Research and Applications (ICRERA), Palermo, 2015, pp. 1631-1634.

[31] P. Li, G. P. Adam, D. Holliday and B. W. Williams, "High power density STATCOM with extended reactive power control range," 2015 International Conference on Renewable Energy Research and Applications (ICRERA), Palermo, 2015, pp. 710-715.

[32] S. F. Panah, T. F. Panah and G. A. Ghannad, "Reactive power compensation in wind power plant with short circuit in power plant line via UPFC," 5th International Conference on Renewable Energy Research and Applications (ICRERA), Birmingham, 2016, pp. 173-176

[33] G. Jung, M. Dinh, H. Sung, J. Lee and M. Park, "Selection and Structural Design of Reactive Power Compensators for a 200 MW Floating Offshore Wind Farm," 8th International Conference on Renewable Energy Research and Applications (ICRERA), Brasov, Romania, 2019, pp. 265-269.